C_{60} on strain-relief patterns of Ag/Pt(111): Film orientation governed by template superstructure

K. Aït-Mansour,* P. Ruffieux, W. Xiao, P. Gröning, R. Fasel, and O. Gröning
Empa, Swiss Federal Laboratories for Materials Testing and Research, nanotech@surfaces Laboratory, Feuerwerkerstrasse 39, CH-3602 Thun, Switzerland

(Received 8 June 2006; revised manuscript received 30 August 2006; published 14 November 2006)

The adsorption, growth and overlayer formation of C_{60} fullerene molecules on strain-relief patterns induced by 2 monolayers of Ag on Pt(111) (Ag(2ML)/Pt(111)) is investigated by means of scanning tunneling microscopy. The Ag(2ML)/Pt(111) template surface consists of periodic crossing dislocations separating face-centered cubic (fcc) and hexagonal close-packed (hcp) stacking domains. At room temperature, C_{60} molecules are found to be sufficiently mobile on the template surface to cross the dislocations and to self-assemble into large hexagonally close-packed two-dimensional islands. The nucleation and growth of the C_{60} islands takes place not only at the step-edges, but also in the middle of terraces. The islands cover as well fcc as hcp domains of the template, in a near commensurate fashion with respect to the Ag(2ML)/Pt(111) superstructure. This commensurability manifests itself by a transfer of the strain relief superstructure into the molecular film via a "lock to register" mechanism. The Ag(2ML)/Pt(111) superstructure acts on the molecular film by orientating the C_{60} close-packed rows along the Ag$\langle 1\bar{1}0\rangle$ direction. This is different from the usual orientation of a C_{60} film on a standard and unreconstructed Ag(111) substrate, namely it is rotated by 30°. The C_{60} "lock to register" phenomenon can find interpretation in a strong substrate-molecule interaction, which can result in a significant compression of the C_{60} lattice. Here, a special role is played by Ag(2ML)/Pt(111) small hcp stacking domains enclosed by strong discommensuration lines, foremost responsible for the "lock to register" mechanism.

DOI: 10.1103/PhysRevB.74.195418 PACS number(s): 81.07.Nb, 81.16.Rf, 81.16.Dn, 68.37.Ef

I. INTRODUCTION

The future of molecular electronics will be crucially depending on the ability to control the assembly of molecular species into complex supramolecular structures. This is true for molecular assembly not only in solutions, but especially also on substrate surfaces. On solid surfaces, there are two major mechanisms which control the self-assembly of molecules. The first mechanism is based on specific and nonspecific molecule-molecule interactions, which can be controlled by an appropriate functionalization of the molecules. This approach has been proven to be successful in the creation of various molecular assemblies, like one-dimensional wires or two-dimensional (2D) molecule lattices, on atomically well defined surfaces,[1,2] as in the case of three-dimensional (3D) assemblies in supramolecular chemsitry.[3] The second mechanism to control the molecular assembly is based on the use of specific molecule-substrate interactions, in other words on the use of template surfaces. However, this approach is by no means trivial because the template lattice parameter should be in the order of the molecule dimensions which typically are in the range 1–2 nm. It is evident that this length scale is still not available to the most advanced micro- or even nano-pattering of semiconductor fabrication like deep UV or electron beam lithography. To obtain substrates structured at the nano-meter scale, new approaches are therefore required. An example of such a new approach is the use of stable vicinal single crystal surfaces like Au(11 12 12), prepared by standard procedures in ultrahigh vacuum (UHV).[4] Here, the combination of the well-known $(22 \times \sqrt{3})$ herringbone reconstruction[5] on small Au(111) terraces with regular steps, induced by the 2.3° miscut of the vicinal Au(11 12 12) surface, leads to the formation of a rectangular 2D pattern of monoatomic steps in one direction and discommensuration lines in the other direction.[4] Another way offering the opportunity to produce nano-structured substrates is the use of heteroepitaxy, as in the case of Ag/Pt(111). In this system, covering clean Pt(111) terraces with 2 monolayers (ML) of Ag [Ag(2ML)/Pt(111)] results in the formation of periodic arrays of crossing dislocations, the so-called dislocation network.[6–11] The dislocations (or more precisely partial dislocations), which are actually discommensuration lines, separate domains of hexagonal close-packed (hcp) termination from domains of face-centered cubic (fcc) termination; this can be compared with the Au(111) herringbone reconstruction.[5]

This paper reports on the adsorption, growth and structural properties of C_{60} thin films deposited at room temperature (RT) on Ag(2ML)/Pt(111) surfaces showing clean and well developed dislocation networks by means of scanning tunneling microscopy (STM). To the best of our knowledge, by now, molecule adsorption on this nano-structured template surface has never been studied. This might be explained by the difficulty to prepare such patterns without the presence of many defects on the surface, as reported in Ref. 6. It is well-known that C_{60} is highly mobile at RT on standard metal surfaces,[12–18] in particular also Ag(111).[13,14] Using STM, here we find that, despite the discommensuration lines of the Ag(2ML)/Pt(111) strain-relief pattern, the molecules are still highly mobile at RT on this surface. Indeed, the C_{60} molecules can cross the dislocation lines, which is evidenced by step-edge decoration by C_{60} before 2D island growth in the middle of terraces begins. The dislocations, however, promote 2D island formation away from the step-edges on the terraces even at low C_{60} coverage. The C_{60} islands on Ag(2ML)/Pt(111) exhibit a well-ordered hcp stacking which is commensurate with the strain-relief pattern. The commensurability of the C_{60} film with Ag(2ML)/Pt(111) pattern can

be understood as a "lock to register" mechanism of the C_{60} lattice with the strain-relief superstructure. This results in the periodicity transferring from the patterned substrate into the C_{60} molecular film which then is rotated by 30° with respect to the usual $(2\sqrt{3}\times 2\sqrt{3})$R30° orientation found on a standard and unreconstructed Ag(111) substrate.[13,14,19] The driving force of this mechanism can be explained by a strong interaction between the Ag(2ML)/Pt(111) dislocation network and the C_{60} molecules.

II. EXPERIMENTAL

We have carried out our investigation of the C_{60} island growth on the dislocation network Ag(2ML)/Pt(111) in two independent UHV systems (base pressure $\sim 1\times 10^{-10}$ mbar) with the same results. The first experiments were conducted with a multi-chamber system equipped with facilities for standard sample preparation (heating and Ar^+ ion sputtering) and housing a commercially available combined STM/AFM (from Omicron) operating at RT. This UHV system also contains chemical characterization techniques, namely a combined setup of X-ray and ultraviolet photoelectron spectroscopy (XPS/UPS), and a crystallographic characterisation instrument which is low energy electron diffraction (LEED) (from Omicron). This UHV system allowed us to monitor the quality and cleanliness of the Ag(2ML)/Pt(111) strain-relief patterns and the subsequent C_{60} depositions. For high resolution STM measurements, we reproduced the experiments in a second UHV system containing a low temperature-(LT-) STM (from Omicron) (operated at 77 K) and a LEED instrument. Similar results were obtained with RT-STM and LT-STM. Here, we only show LT-STM measurements, as they are of a better quality. Polycrystalline Pt/Ir (80/20) wire was used for STM tips. The STM images presented in this paper were recorded in the constant current mode, the stated bias voltage refers to the electric potential of the sample with respect to the tip.

The Pt(111) single-crystal (disk of 8 mm diameter, 2 mm thickness) used throughout this study was delivered from MaTeck Corporation. The Pt(111) substrate was first cleaned by several cycles of Ar^+ sputtering (at 1 keV) at RT and subsequent heating at 850 °C, the temperature being monitored by an infrared pyrometer. Then, the Pt(111) substrate was exposed to Ar^+ sputtering at the temperature of 850 °C. This preparation procedure enabled us to remove any trace of impurities (checked by XPS) and to obtain a very sharp (1 $\times$1) LEED pattern. STM measurements of such a clean Pt(111) showed large terraces ($\sim$150 nm width, which sometimes well exceeded 200 nm), separated by 2.3 Å monoatomic steps. These large terraces are well suited for the formation of Ag(2ML)/Pt(111) dislocation networks with a long-range order. Ag (shots of 1–5 mm diameter, purity =99.99%, from Alfa Aesar) was sublimated from a home-built evaporator using electron-bombardment heating. The employed Ag evaporation rate of $\sim$0.5 ML per minute was monitored by a water-cooled quartz microbalance and also systematically controlled with STM. Here, one ML Ag refers to the completion of a closed atomic layer on Pt(111), as estimated with STM. To produce Ag(2ML)/Pt(111) patterns on a large scale, Ag was first deposited at RT; the Ag coverage was slightly lower than 2 ML in order to avoid Ag clusters on the surface, that would form at a coverage of more than 2 ML (even if the Ag excess is very minute). The evaporated Ag film was subsequently annealed (for 5 minutes) at 530 °C, as reported in literature.[6–11]

Once the quality and cleanliness of the Ag(2ML)/Pt(111) pattern was checked by STM, C_{60} molecules were deposited onto the sample kept at RT. The C_{60} molecular beam was generated from a Knudsen effusion cell, using a stainless steel crucible containing C_{60} powder heated at $\sim$400 °C, toped by a small opening which limits the sublimating molecules to a narrow solid angle. Our C_{60} deposition rate, monitored by a quartz microbalance and calibrated by STM, was in the order of 0.05 ML/min. One C_{60} ML coverage corresponds to a single complete close-packed layer of molecules observed with STM. Different C_{60} coverages were deposited at RT on Ag(2ML)/Pt(111) patterns and then measured by RT-STM and LT-STM. The data presented in this paper are related to a C_{60} film of 0.4 ML deposited at RT and analyzed with LT-STM (at 77 K).

III. RESULTS AND DISCUSSION

A. Strain-relief pattern Ag(2ML)/Pt(111)

It has been reported in literature[7] that Ag deposition at RT on Pt(111) follows the Stranski-Krastanov growth mode, namely initial 2D- followed by 3D-growth, with a critical film thickness of 6–9 ML (corresponding to the 2D-3D transition). In our case (film thickness $\sim$2 ML), Ag is thus expected to grow layer-by-layer. We have found using STM (images not shown) that this is in fact the case, as the Ag deposition at RT results in a nearly perfectly closed 2 ML film on which some occasional Ag 2D islands can be observed. LEED analysis of the Ag deposition shows a hexagonal spot pattern (not depicted here) indicating that Ag grows along its $\langle 111\rangle$ axis (with $\mathrm{Ag}\langle 1\bar{1}0\rangle \| \mathrm{Pt}\langle 1\bar{1}0\rangle$). The as-observed layer-by-layer growth of Ag on Pt(111) is due the considerable mobility of the Ag adatoms even at RT. This growth mode is also predicted by the well-known Bauer's criterion which gives a large negative difference between the surface free energy of Ag(111) (adsorbate) and that of Pt(111) (substrate): $\gamma_{\mathrm{Ag}(111)}$-$\gamma_{\mathrm{Pt}(111)}\sim -0.5$ eV per atom (see, e.g., Ref. 7 and references therein). Moreover, previous works[6–10] have demonstrated that the first ML of Ag on Pt(111) grows pseudomorphically, under an isotropic compressive strain of 4.3%, while the higher layers (2-3) relax via the formation of a dislocation network.

In order to achieve long-range domains of the dislocation network Ag(2ML)/Pt(111), the Ag film deposited at RT was heated at 530 °C. The surface morphology after this annealing step is shown on the STM images of Fig. 1(a) and 1(b). One can see that the surface exhibits a very well-defined superstructure induced by crossing dark lines which precisely are dislocation domains. By the preparation procedure described above, we achieve extended ($>$100 nm $\times$100 nm) high quality dislocation networks, whose STM images are comparable with the best one published for this

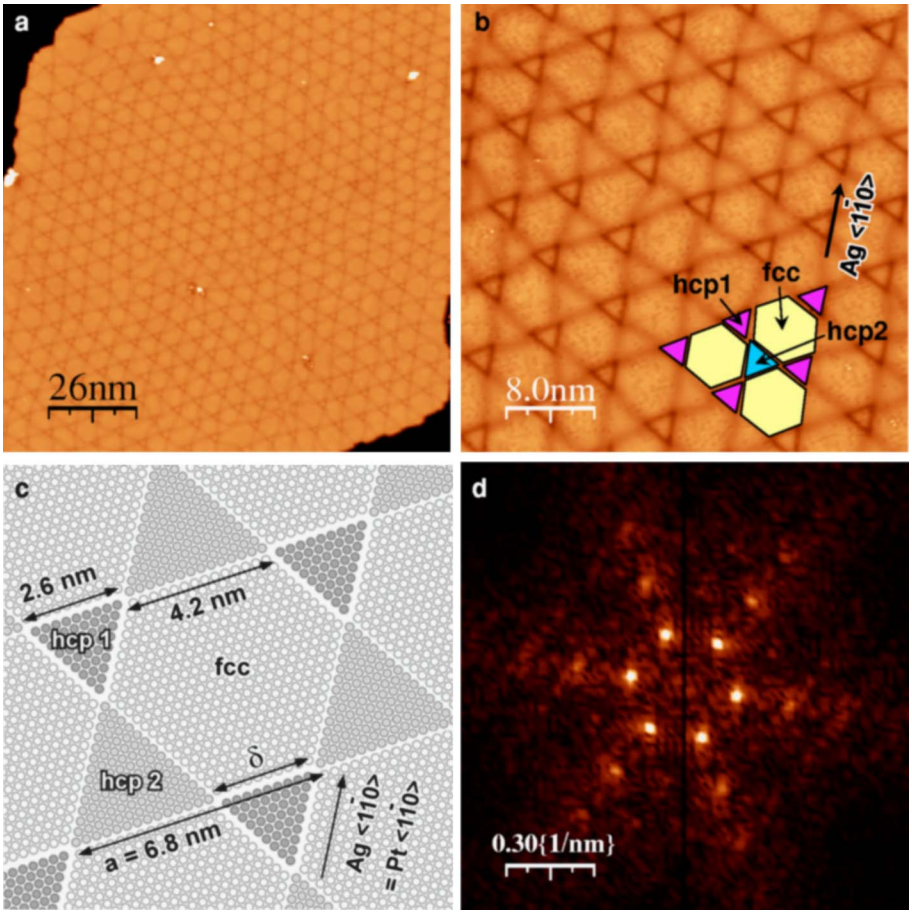

FIG. 1. (Color online) Topographic LT-STM images (2 nA, −2 V) (a) 130 nm×130 nm and (b) 40 nm×40 nm showing an Ag(2ML)/Pt(111) strain-relief pattern [(b) is a detail of (a)]. (c) A schematized top view of some unit cells of the Ag(2ML)/Pt(111) dislocation network superstructure shown in (a,b). The circles represent Ag atoms (model after Refs. 6 and 9, see text). It is not clear, however, if the dislocations are present in the topmost Ag layer or are buried in the first Ag layer on the Pt(111) substrate. (d) FFT spectrum of image (b) illustrating the hexagonal symmetry of the Ag(2ML)/Pt(111) superstructure.

surface so far.[9] However, from Fig. 1(a), it is evident that some small clusters (white spots on the STM image) remain on the surface. These clusters have a mean height of about 2–3 Å and are attributed to Ag clusters[11] whose diffusion to the step edges is hindered by the strain-relief network or defects in the same.

The close-up of the strain relief pattern shown on the STM image in Fig. 1(b) evidences a hexagonal symmetry which is also readily observed on the corresponding fast Fourier transform (FFT) displayed in Fig. 1(d). Both STM images in Fig. 1(a) and 1(b) and FFT spectrum in Fig. 1(d) give an average period of the network of a=6.8 nm. The strain-relief pattern describes a hexagonal superstructure which then can be estimated to be a (24×24) Ag unit cell, as a=6.8 nm is very close to $24\times a_{Ag}/\sqrt{2}=6.9$ nm, or, with respect to the Pt(111) substrate, (25×25) Pt unit cell, with $25\times a_{Pt}/\sqrt{2}=6.9$ nm ($a_{Ag}=4.085$ Å and $a_{Pt}=3.924$ Å). The as-deduced approximate surface reconstruction also agrees with that of (25×25) associated by Brune *et al.* to the Ag(2ML)/Pt(111) strain-relief network.[9] However, as can be clearly seen on Fig. 1(a) and 1(b), the network is not absolutely regular as locally the lattice parameter can vary between 6 and 8 nm. This imperfect regularity is typical for the Ag(2ML)/Pt(111) dislocation networks and can be observed on all STM images of this surface published so far.[6–11]

Let us now see the details of the dislocation network shown on the STM images in Fig. 1(a) and 1(b) and whose some unit cells are drawn in Fig. 1(c). This gives a schematic atomic illustration of the strain-relief superstructure; here a structure of (24×24) Ag unit cell has been assumed. It is not clear, at this stage, if the dislocations are present in the top Ag layer or are buried in the first Ag layer on the Pt(111) substrate. An atomic model of the Ag(2ML)/Pt(111) dislocation network has been proposed by Brune *et al.*[6] According to this model, the unit cell (see Fig. 1(b) and 1(c)) contains one hexagon (with irregular side length) with Ag atoms in a fcc stacking sequence, one smaller triangle (hcp1) and one bigger triangle (hcp2), both with Ag atoms in a hcp stacking sequence. The edges of the fcc hexagons are aligned along the $\langle 1\bar{1}0\rangle$ directions of the (111) plane of Ag (and Pt). One can clearly observe on Fig. 1(b) and 1(c) two inequivalent borders separating a given fcc hexagon from the two hcp type triangles. Indeed, there are three long borders with the three nearest-neighbor big triangles (hcp2) and three short borders with the three nearest-neighbor small triangles (hcp1). The long fcc-hcp2 walls are simple transitions from

fcc to hcp stacking[6] and appear slightly lower in the STM image in Fig. 1(b). The short fcc-hcp1 walls correspond to Ag atoms occupying bridge sites.[6] These walls have a lower atomic density than the fcc-hcp2 walls and appear lower, as darker lines, in the STM image in Fig. 1(b). We have estimated the offset δ (see Fig. 1(c)), which is the edge length of an hcp1 stacking triangle, to be 2.6 nm for a period a =6.8 nm. The δ/a ratio is then 0.38, close to the values already given by other authors: 0.3 (Ref. 6) and 0.4 (Ref. 11). Our STM measurements also show that Ag atoms of the deep dislocation regions (darker lines) are 0.25 Å lower than Ag atoms situated in the centre of the nearest hcp1 stacking domain. Regarding this strain-relief pattern, in their works,[9,10] Brune *et al.* have attributed two different energy barriers, on the one hand for Ag adatom diffusion within one fcc (or hcp) stacking and on the other hand for Ag adatom diffusion across the dislocations marking transitions from fcc to hcp stacking. The dislocations have been found to have much higher diffusion barrier (2–3 times) than a fcc (or hcp) stacking domain for Ag adatom diffusion.

B. Adsorption, growth and structure of C_{60} on strain-relief patterns Ag(2ML)/Pt(111)

In this section, we now investigate the adsorption at RT of C_{60} cages on the reconstructed surface Ag(2ML)/Pt(111). STM analysis of a C_{60} thin film of about 0.08 ML coverage (not presented here) revealed that the C_{60} molecules were adsorbed at step-edges without any formation of 2D C_{60} island in the middle of terraces. This indicates (i) the high mobility of the C_{60} molecules at RT,[12–18] (ii) the higher molecule absorption energy at the steps compared to the bare terraces[12,13,15–18] and (iii) that at RT the C_{60} cages are able to cross the strain-relief discommensuration lines. Figures 2 and 3 show STM measurements of a 0.4 ML C_{60} film deposited at RT on Ag(2ML)/Pt(111). The estimation of the film coverage was based on different large 500 nm × 500 nm STM images taken from various zones on the sample. A typical large area STM picture of the C_{60} film showing four substrate terraces with three step-edges is displayed in Fig. 2(a). As can be seen on this image, and on a detail image in Fig. 2(b), the step-edges are fully decorated by C_{60} 2D islands and some C_{60} linear chains. In addition to the island growth at the step-edges, Fig. 2(a) also clearly shows nucleation of big islands in the middle of terraces, with typical diameters ranging between 20 and 70 nm. We have observed that C_{60} 2D islands start to grow on terraces only when the step-edge sites are fully decorated. Typical C_{60} islands nucleated in the middle of a terrace are displayed on the STM images in Fig. 3(a) and 3(b). These images show that the C_{60} islands are adsorbed on both fcc and hcp stacking domains of the strain-relief pattern and are extended over several unit cells of Ag(2ML)/Pt(111). The molecules landing on hcp domains can then diffuse into fcc domains and vice versa. The well-established repulsive character of the crossing dislocations,[9,10] which dominates at 110 K for metal (Ag) deposition, is in the present case not sufficiently strong to prevent significant molecule diffusion across the discommensuration lines from fcc sites into hcp ones at RT.

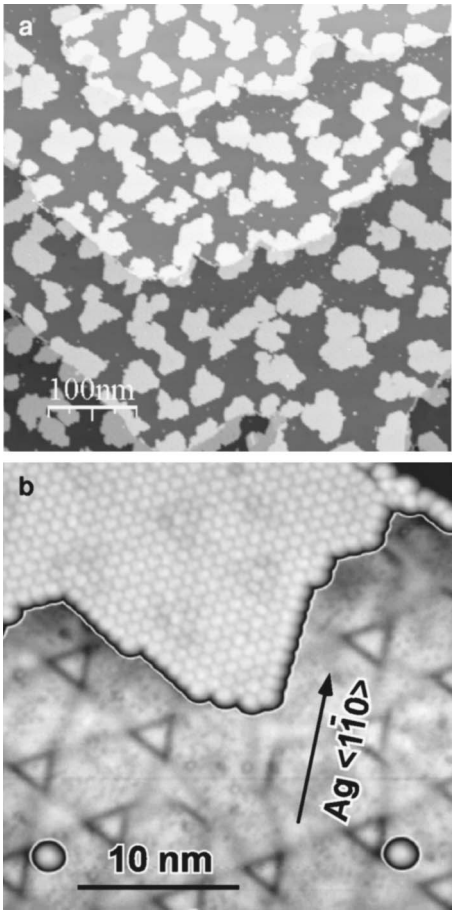

FIG. 2. Topographic LT-STM images (0.01 nA, −2 V) illustrating the adsorption at RT of 0.4 ML C_{60} on the Ag(2ML)/Pt(111) strain-relief pattern: (a) 500 nm × 500 nm, (b) 28 nm × 28 nm. (b) displays a C_{60} 2D island at a step edge and two isolated C_{60} molecules in touch with Ag(2ML)/Pt(111) deep dislocations. In (b), a dual tone gray scale has been chosen to allow the visualization of the molecules and the substrate dislocation network.

In addition to the C_{60} 2D islands, individual C_{60} cages (see Fig. 2(b)) as well as aggregates of a few molecules (see the three dark isolated clusters in Fig. 3(a)) are also present at the surface. It is noteworthy to observe that some isolated molecules are stable in the middle of terraces when deposited at RT. This single molecule stability was also confirmed by putting, after a first LT-STM investigation, the sample at RT for two days, and after that analysing the sample again a second time at 77 K. We have then observed that individual molecules are still located at identical sites on the surface (as for the two molecules shown in Fig. 2(b)). This observation indicates that at RT the thermal energy is just sufficient to allow the majority of molecules to diffuse across the dislocation network and agglomerate into islands. As is evident from Fig. 2(b), the individual C_{60} molecules are pinned near the hcp smaller triangles of the strain-relief network, in touch with the deep dislocations. This is comparable to the adsorption of Ag clusters on Ag(2ML)/Pt(111)[11] and can be explained by a higher diffusion barrier corresponding to these deep dislocations.[9,10] It should also be noted that a preferential adsorption of individual C_{60} molecules near dislocations

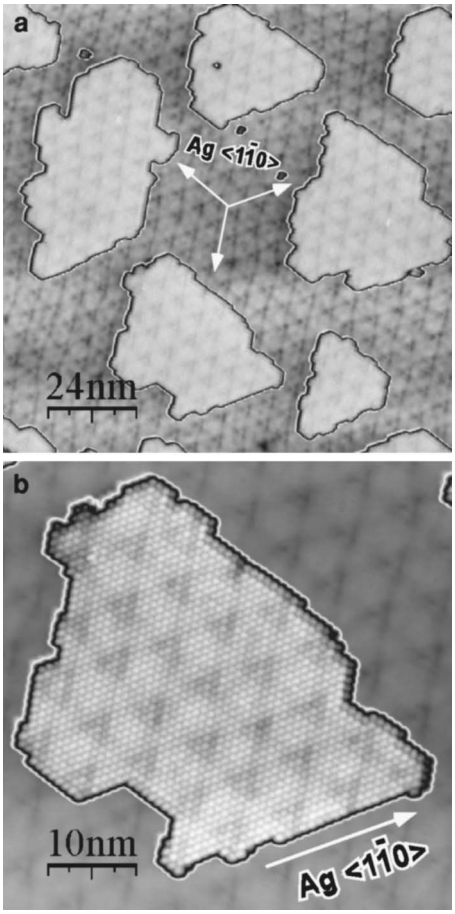

FIG. 3. LT-STM images (0.01 nA, −2 V) (a) 120 nm × 120 nm and (b) 50 nm × 50 nm showing C_{60} 2D islands grown in the middle of an Ag(2ML)/Pt(111) terrace. ((a) is a detail measured on the upper part of Fig. 2(a).) The Ag(2ML)/Pt(111) superstructure is clearly imprinted in the C_{60} 2D islands. In both images (a) and (b), a dual tone gray scale has been chosen to allow a better visualisation of the C_{60} triangular features (or/and the C_{60} lattice) and the substrate dislocation network superstructure.

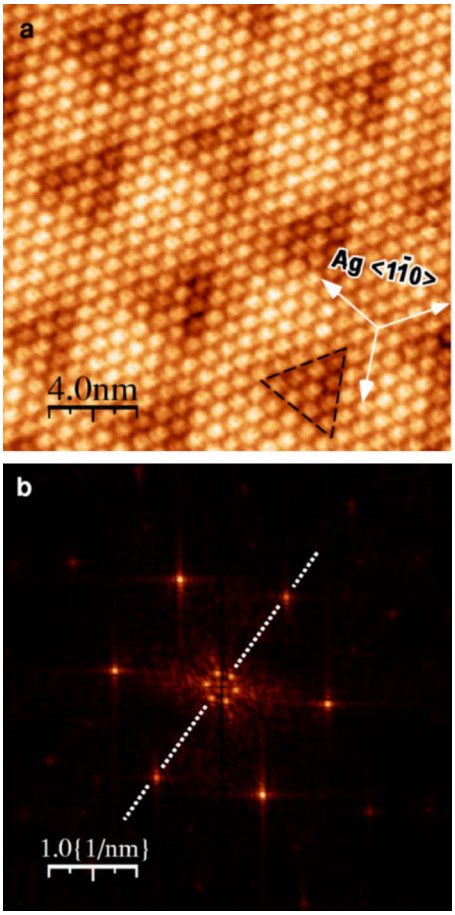

FIG. 4. (Color online) (a) High resolution LT-STM image (0.01 nA, −2 V) 20 nm × 20 nm measured on the C_{60} 2D island displayed on the image 3.(b). Highlighted triangular features (containing 10 C_{60} molecules) fingerprint the transfer of the Ag(2ML)/Pt(111) superstructure to the C_{60} film. (b) FFT spectrum of image (a) showing two spot hexagons: the big one corresponds to the C_{60} hcp stacking and the small one is related to the substrate superstructure transferred to the molecular film, as attested by the triangular features. The coincidence in the orientation of the two spot hexagons indicated by a dotted line in (b) shows that the C_{60} close-packed rows are aligned along the Ag$\langle 1\bar{1}0\rangle$ direction.

has also been observed on an Au(001) reconstructed surface as well.[20]

Figures 2 and 3 show that the C_{60} molecules of the 0.4 ML film in majority self-assemble to form well-ordered phases that are crystalline 2D islands. This island formation is governed by the in-plane hcp stacking of the C_{60} molecules. We now want to examine the orientation of the C_{60} molecule rows with respect to the strain-relief pattern Ag(2ML)/Pt(111). The STM images of Figs. 2 and 3 exhibit C_{60} islands with close-packed rows parallel to that of Ag(111) (namely the Ag$\langle 1\bar{1}0\rangle$ directions). One can also note that the C_{60} islands are delimited by borders which are mostly parallel to their close-packed rows. This orientation of the islands has been found to be dominant in our case and this has also been confirmed by LEED, a technique which is well-known to give, via the reciprocal space, statistical information from much larger area than those probed with STM. As shown on STM images in Fig. 2(b) and Fig. 3(a) and 3(b), this orientation allows the near commensurate transfer of the Ag(2ML)/Pt(111) superstructure to the molecular film via a mechanism which we describe as a "lock to register", fingerprinted by triangular features. The "lock to register" mechanism with the orientation of C_{60}-C_{60} rows along Ag$\langle 1\bar{1}0\rangle$ is well displayed on the high resolution STM image in Fig. 4(a) (measured on the island displayed in Fig. 3(b)) and its FFT spectrum in Fig. 4(b). A schematic structural representation of the C_{60} film orientation on Ag(2ML)/Pt(111) is shown on Fig. 5(a).

We now focus on the molecules located on the hcp1 stacking small triangles whose edges correspond to the deep dislocations of the patterned substrate. These triangular features (highlighted on Fig. 4(a)) consist of 10 C_{60} molecules, 1 central molecule and 9 peripheral ones (see also Fig. 5(a)). As seen on one triangular feature measured with STM, the central molecule is imaged with higher apparent height, roughly 0.15 Å higher than the 9 peripheral ones. One can then reasonably understand that the 9 peripheral C_{60} cages

are locking into the three strong fcc-hcp1 discommensuration lines and that the central C_{60} cage occupies the centre of the hcp1 triangle, as schematized on Fig. 5(a). The molecular corrugation of 0.15 Å is to be compared to the height difference of about 0.25 Å between the centre of an hcp1 stacking small triangle and one corresponding deep dislocation in the case of the Ag(2ML)/Pt(111) strain-relief pattern (see section III.A). The apparent difference of 0.1 Å between the substrate and molecule corrugations may be explained by the fact that the 9 peripheral C_{60} molecules are not located exactly on the deep dislocations, but just near and in contact with them, slightly outside the hcp1 small triangle. This argument can be drawn if one compares the triangular features visible on the C_{60} film (Fig. 4(a)) to those observed on the Ag(2ML)/Pt(111) pattern (Fig. 1(b)). Then, one can easily see that they are larger in the case of the C_{60} film.

The molecular film orientation found here, with the C_{60} close-packed rows parallel to that of Ag ($\langle 1\bar{1}0\rangle$), is not usual. Indeed, the growth of C_{60} films on an unreconstructed Ag(111) substrate leads to C_{60} close-packed rows rotated by 30° compared to Ag$\langle 1\bar{1}0\rangle$ direction (i.e., parallel to Ag$\langle$11–2$\rangle$).[13,14,19] This situation results from the fact that the C_{60} monolayer film on the unreconstructed Ag(111) surface adopts a $(2\sqrt{3}\times 2\sqrt{3})$R30° structure[13,14,19] which can be explained by the very good lattice matching between the hcp stacking of C_{60} cages and the Ag(111) substrate lattice: $2\times\sqrt{3}\times a_{Ag}/\sqrt{2}=10.0$ Å$=C_{60}$-C_{60} distance. The as-reported $(2\sqrt{3}\times 2\sqrt{3})$R30° orientation, schematized on Fig. 5(b), can also be found on our samples, however only very seldom and for small islands. Such a C_{60} molecular film orientation, with the C_{60}-C_{60} rows parallel to the $\langle$11-2$\rangle$ direction of the substrate, has also been found on the (111) surface of Al.[15,21,22] The structural similarity of C_{60} films on Ag(111) and Al(111) is not surprising as there is only a slight lattice mismatch of 1% between the two substrates and both do not reconstruct (in the absence of adsorbates). Moreover, Altman and Colton have undertaken a comparative STM study on C_{60} growth on Au(111) and Ag(111).[12–14] C_{60} ML on Au(111) shows an orientation of the hcp lattice rotated by 30° compared to the $(2\sqrt{3}\times 2\sqrt{3})$R30° orientation on Ag(111). As Au(111) and Ag(111) are very similar with regard to lattice parameter and electronic structure, the difference in the orientation of the C_{60} layer has been attributed to the $(22\times\sqrt{3})$ superstructure of Au(111).[12–14] The system C_{60}/Ag(111) as well C_{60}/Au(111) obeys the general trend of C_{60} on metal surfaces where the molecule-substrate interaction is better described as chemisorption (strong) bonding (see, for instance, Refs. 12–16 and 18–22 and references therein) rather than van der Waals (weak) bonding which is characteristic of C_{60} fcc solid.

In our present system, there are key-observations which unambiguously indicate that the interaction between the Ag(2ML)/Pt(111) strain relief pattern and the C_{60} cages is strong: (i) the growth of well-ordered hexagonally close-packed 2D islands in the middle of terraces, (ii) the unusual orientation of the C_{60} film with close-packed rows along Ag$\langle 1\bar{1}0\rangle$ and (iii) the transfer of the substrate strain-relief superstructure to the C_{60} overlayer. Another argument in the same line is given by heating a C_{60} film (lower than, or equal to, 1 ML) at 530 °C. We have found, using XPS and STM, that this annealing procedure does not reduce the C_{60} amount at the surface. Thus, at 530 °C C_{60} molecules do not desorb from the substrate surface, while their temperature of sublimation from a C_{60} powder is only of ~400 °C. Another element supporting the strong substrate-molecule interaction in our case is given by the short distance between two nearest-neighbor C_{60} molecules. This distance is estimated (with the image 4.(a) and the corresponding FFT spectrum in Fig. 4(b) and with other STM measurements) to be of about 9.3 Å. However, this value can vary from C_{60} island to C_{60} island in the range between 9.3 Å and 10.0 Å. It has to be reiterated here that the Ag(2ML)/Pt(111) dislocation network is not strictly regular and the C_{60}-C_{60} distance depends on the local lattice parameter of the Ag(2ML)/Pt(111) superstructure. The 9.3 Å C_{60}-C_{60} intermolecular distance discussed here represents the lower extreme value found for the C_{60} films on the Ag(2ML)/Pt(111) and is significantly lower than the usual one (of 10.0 Å) found in the C_{60} bulk crystal, C_{60} multilayers or even in C_{60} thin films. One may notice that our 9.3 Å C_{60}-C_{60} distance is between the C_{60} hard-sphere diameter (7.1 Å) and the nearest-neighbor distance (10.0 Å) in C_{60} fcc crystal. The short intermolecular distance

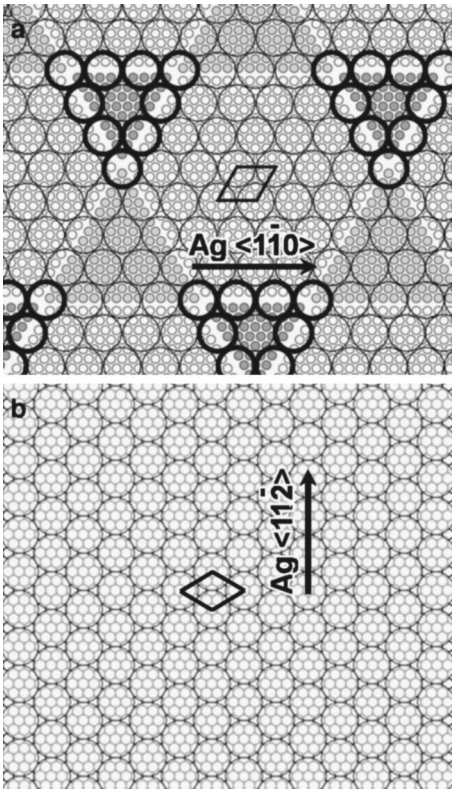

FIG. 5. (a) Schematic representation of C_{60} film orientation on Ag(2ML)/Pt(111) governed by the template superstructure, i.e., with C_{60}-C_{60} close-packed rows along Ag$\langle 1\bar{1}0\rangle$. Comparison with (b) C_{60} monolayer orientation on a standard and unreconstructed Ag(111) substrate with C_{60}-C_{60} close-packed rows aligned along Ag$\langle 11\bar{2}\rangle$ and which gives rise to a $(2\sqrt{3}\times 2\sqrt{3})$R30° structure.[13,14,19] The small and big circles represent Ag atoms and C_{60} molecules, respectively, in both models (a) and (b).

indicates that the C_{60} is under high compressive stress (7%). One can therefore reasonably admit that a strong driving force is exerted by the Ag(2ML)/Pt(111) pattern on the C_{60} molecules for their adsorption into specific sites. Let us recall that compression and expansion are possible in C_{60} films on metal surfaces, depending on the substrate and its crystallographic symmetry, on which the molecules are deposited, as previously reported by many studies.[15,19,20,22–24] However, from these studies, one might notice that the C_{60} films usually are more susceptible to expansion (up to 11–12%[23,24]) than compression. The previous works[15,19,20,22–24] also indicate that the compression generally does not exceed 4% (intermolecular distance of 9.6 Å), except only for one case where the smallest intermolecular distance reported up to now is 8.0 Å (compression=20%).[20] This high compression has been obtained on a reconstructed Au(001) surface and has been found to be uniaxial. In our case the C_{60} film compression seems to be isotropic, which can be understood from the hexagonal symmetry of the Ag(2ML)/Pt(111) dislocation pattern. The 7% high compression of the C_{60} ordered self-assembly must be induced by the strain-relief superstructure of the Ag(2ML)/Pt(111) pattern, as on Ag(111) substrate no such compression has been observed.[13,14] Furthermore, the C_{60} compression must also be closely related to the "lock to register" mechanism of the C_{60} lattice with the substrate reconstruction and must result from a strong substrate-molecule interaction. In terms of electrons, the strong substrate-molecule interaction may be explained by a charge transfer from the substrate into the low unoccupied molecular orbital band of the C_{60} molecules. Such a charge transfer, even if differing from substrate to substrate, is common for C_{60} on metal surfaces.[14,18–20,22,25] It should be interesting to examine with UPS a monolayer system such as 1 ML C_{60}/Ag(2ML)/Pt(111) in order to point out a spectroscopic signature of the molecule-substrate interaction. Referring to the structural model presented in Fig. 5(a), we can see that, among the 49 C_{60} molecules covering a unit cell of the dislocation network, 3 C_{60} are located in a corner position and 6 C_{60} in an edge position of the dislocations surrounding an hcp1 domain. It seems that the gain in adsorption energy of these 9 among 49 molecules is sufficient to induce the unusual orientation of the whole C_{60} film.

IV. CONCLUSION

This paper was devoted to study for the first time molecule (C_{60}) adsorption on the stain-relief pattern of Ag(2ML)/Pt(111) using STM. We succeeded in producing large Ag(2ML)/Pt(111) template terraces (exceeding 100 nm) of high quality, suitable for molecule adsorption experiments. We have shown that the C_{60} molecules are of high mobility at RT on Ag(2ML)/Pt(111) and able to cross the substrate dislocations, which is indicated by a complete step-edge decoration at low molecule coverage (0.08 ML). At higher coverage (0.4 ML), island formation, at the step-edges but also on the bare strain-relief network, could be observed. The C_{60} islands extent over both fcc and hcp stacking domains of the strain-relief pattern Ag(2ML)/Pt(111). With hexagonally close-packed C_{60} lattice, the 2D islands exhibit an ordered phase which grows near commensurably on the Ag(2ML)/Pt(111) superstructure. Clearly, substrate triangular features visible through the C_{60} islands are the fingerprint of C_{60} commensurability on Ag(2ML)/Pt(111). This commensurability has been identified as a "lock to register" mechanism of the C_{60} lattice with the strain-relief superstructure. This "lock to register" mechanism implies an orientation of the C_{60} close-packed rows along Ag$\langle 1\bar{1}0\rangle$, i.e., rotated by 30° compared to the usual orientation found in literature on the unreconstructed Ag(111) substrate. The interaction of the C_{60} overlayer with the strain-relief network seems to be sufficiently strong to induce occasionally a significant compression of the C_{60} lattice of up to 7%. The "lock to register" mechanism is an indication of a first step of adsorption/assembly selectivity of C_{60} cages on the Ag(2ML)/Pt(111) strain-relief pattern. In this same line, further investigations are under way.

ACKNOWLEDGMENTS

This work was financially supported by the European Commission (RADSAS, NMP3-CT-2004-001561).

*Corresponding author: Kamel Aït-Mansour, Empa, Swiss Federal Laboratories for Materials Testing and Research, nanotech@surfaces Laboratory, Feuerwerkerstrasse 39, CH-3602 Thun, Switzerland; E-mail: Kamel.Ait-Mansour@empa.ch; Tel: +41 (0)33 228 29 32; Fax: +41 (0)33 228 44 90

[1] T. Yokoyama, S. Yokoyama, T. Kamikado, Y. Okuno, and S. Mashiko, Nature **413**, 619 (2001).
[2] J. A. Theobald, N. S. Oxtoby, M. A. Phillips, N. R. Champness, and P. H. Beton, Nature **424**, 1029 (2003).
[3] J.-M. Lehn (VCH, Weinheim, 1995); J.-M. Lehn, Rep. Prog. Phys. **67**, 249–265 (2004).
[4] N. Witkowski, Y. Borensztein, G. Baudot, V. Repain, Y. Girard, and S. Rousset, Phys. Rev. B **70**, 085408 (2004); W. Xiao, P. Ruffieux, K. Aït-Mansour, O. Gröning, K. Palotas, W. A. Hofer, P. Gröning, and R. Fasel, J. Phys. Chem. B **110**, 21394 (2006).
[5] J. V. Barth, H. Brune, G. Ertl, and R. J. Behm, Phys. Rev. B **42**, 9307 (1990).
[6] H. Brune, H. Röder, C. Boragno, and K. Kern, Phys. Rev. B **49**, 2997 (1994).
[7] H. Röder, K. Bromann, H. Brune, and K. Kern, Surf. Sci. **376**, 13 (1997).
[8] K. Bromann, H. Brune, M. Giovannini, and K. Kern, Surf. Sci. **388**, L1107 (1997).
[9] H. Brune, M. Giovannini, K. Bromann, and K. Kern, Nature **394**, 451 (1998).
[10] H. Brune, Surf. Sci. Rep. **31**, 121 (1998).
[11] H. Jödicke, R. Schaub, R. Monot, J. Buttet, and W. Harbich, Surf. Sci. **475**, 109 (2001).

[12] E. I. Altman and R. J. Colton, Surf. Sci. **279**, 49 (1992).
[13] E. I. Altman and R. J. Colton, Surf. Sci. **295**, 13 (1993).
[14] E. I. Altman and R. J. Colton, Phys. Rev. B **48**, 18244 (1993).
[15] M. K.-J. Johansson, A. J. Maxwell, S. M. Gray, P. A. Brühwiler, and L. S. O. Johansson, Surf. Sci. **397**, 314 (1998).
[16] E. Giudice, E. Magnano, S. Rusponi, C. Boragno, and U. Valbusa, Surf. Sci. **405**, L561 (1998).
[17] M. Abel, A. Dimitriev, R. Fasel, N. Lin, J. V. Barth, and K. Kern, Phys. Rev. B **67**, 245407 (2003).
[18] C. Silien, N. A. Pradhan, W. Ho, and P. A. Thiry, Phys. Rev. B **69**, 115434 (2004).
[19] M. Pedio, K. Hevesi, N. Zema, M. Capozi, P. Perfetti, R. Gouttebaron, J.-J Pireaux, R. Caudano, and P. Ruolf, Surf. Sci. **437**, 249 (1999).
[20] Y. Kuk, D. K. Kim, Y. D. Suh, K. H. Park, H. P. Noh, S. J. Oh, and S. K. Kim, Phys. Rev. Lett. **70**, 1948 (1993).
[21] R. Fasel, P. Aebi, R. G. Agostino, D. Naumovic, J. Osterwalder, A. Santaniello, and L. Schlapbach, Phys. Rev. Lett. **76**, 4733 (1996).
[22] M. K.-J. Johansson, A. J. Maxwell, S. M. Gray, P. A. Brühwiler, D. C. Mancini, L. S. O. Johansson, and N. Mårtensson, Phys. Rev. B **54**, 13472 (1996).
[23] R. Fasel, R. G. Agostino, P. Aebi, and L. Schlapbach, Phys. Rev. B **60**, 4517 (1999).
[24] J. Weckesser, C. Cepek, R. Fasel, J. V. Barth, F. Baumberger, T. Greber, and K. Kern, J. Chem. Phys. **115**, 9001 (2001).
[25] G. K. Wertheim, D. N. E. Buchanan, Phys. Rev. B **50**, 11070 (1994); L. H. Tjeng, R. Hesper, A. C. L. Heessels, A. Heeres, H. T. Jonkman, and G. A. Sawatzky, Solid State Commun. **103**, 31 (1997).